Optimization of magnesium oxychloride cement formation using experimental design methodology

Amal Brichni [a,b], Halim Hammi [a], Salima Aggoun [c], Adel Mnif [a]

[a)] *Useful Material valorization laboratory, National Center for Research in Materials Sciences, Technopole Borj Cedria, BP73, 8027 Soliman-Tunisia;*
[b)] *Université de Tunis El Manar, Faculté des Sciences de Tunis, 2092, Tunis, Tunisie.*
[c)] *University of Cergy-Pontoise (L2MGC), 5 Mail Gay-Lussac, Neuville Sur Oise, 95000 Cergy-Pontoise Cedex, France;*

(Received : 17 February 2016, accepted: 05 April 2016)

Abstract: In this work, the experimental design methodology is applied to optimize the condition of formation of Magnesium chloride cement. A four factors factorial design to model and to optimize the operating parameters that govern the formation was used. The studied factors were mass ratio of $MgCl_2.6H_2O/MgO$, mixing time and stirring speed. Considered responses are compressive strength and setting time. The optimum operating conditions were quite efficient to have a good compressive strength and suitable setting time. The phases compositions of magnesium oxychloride cement were evaluated by X-ray diffraction, the morphological properties were examined by SEM and their thermal behaviour was analyzed by DTA/TGA. The presence of phase 5 confirms the good compressive strength of magnesium oxychloride cement.

Keywords: Magnesium oxychloride cement, Experimental design methodology, Optimization.

INTRODUCTION

Magnesium chloride cement (MOC) has superiors properties as compared to ordinary Portland cement such as high compressive strength [1], good resistance to abrasion, rapid hardening rate, good cohesiveness, high fire resistance [2] and it can be use with all kinds of aggregates [3]. The main used applications are architectural such as construction of industrial floors, construction of thermal and acoustical insulating panels [4] and other prefabricated building boards [5]. The basic chemical reaction system of MOC system is $MgO–MgCl_2–H_2O$ [6-7]. The main bonding phases found in hardened MOC are $5Mg(OH)_2.MgCl_2.8H_2O$ (phase5) and $3Mg(OH)_2.MgCl_2.8H_2O$ (phase 3) which are obtained by the following chemical reactions[7]:

$$5MgO + MgCl_2 + 13\ H_2O = 5Mg(OH)_2.MgCl_2 + 8\ H_2O \quad (1)$$

$$3MgO + MgCl_2 + 11\ H_2O = 3Mg(OH)_2.MgCl_2 + 8\ H_2O \quad (2)$$

They are the only stable phases in the system $MgO\text{-}MgCl_2\text{-}H_2O$. Due to the presence of excess water a parallel or competitive reaction, corresponding to the magnesium oxide hydration can take place:

$$MgO + H_2O = Mg(OH)_2 \quad (3)$$

The presence of $Mg(OH)_2$ indicates the low quality of the magnesium oxychloride cement.

Furthermore, the widespread use of magnesium oxychloride cement has been limited because of loss of strength on prolonged excessive exposure to water [8]. Much research has long been processed to improve the water-resistance of magnesium oxychloride based on his ability to the binding of various organic and inorganic aggregates such as high active SiO_2 [9-10], active aluminates [1] sulfates and phosphoric acid or phosphate [12].

In this work, the influence of three factors (mass ratio of $MgCl_2/MgO$, mixing time and

* Corresponding author, e-mail address : amal.brichni@gmail.com, halimhammi2015@gmail.com, salima.aggoun@u-cergy.fr, mnifinrst@gmail.com

Table I: Chemical compositions of the used raw materials

MgO	**Component**	**MgO**	**ClO_2**	**SO_4**	**CaO**	**Heavy metal (as Pb)**	**Fe_2O_3**	**CuO**
	Mass fraction (%)	98.0	0.01	0.001	0.02	0.001	0.005	0.01
$MgCl_2.6H_2O$	Component	$MgCl_2.6H_2O$	SO_4	As_2O_3	$CaCl_2$	Fe_2O_3	K_2O	NaCl
	Mass fraction (%)	99.0	0.002	0.0002	0.003	0.0005	0.001	0.001

stirring speed) on compressive strength and setting time of MOC was carried out. The application of the experimental design methodology was used in order to maximize synthesis yield by searching for the optimum experimental conditions in a less number of experiments.

MATERIAL AND EXPERIMENTAL PROCEDURE

1. Materials

The raw materials used in the study were magnesium oxide and magnesium chloride hexahydrate. The magnesium oxide was produced by HIMEDIA (Laboratories in India) and magnesium chloride hexahydrate was produced by Scharlab in Spain. The chemical compositions of the raw materials are listed in table I.

2. Preparation of magnesium chloride solution:

Saturated Magnesium chloride solution was prepared by dissolving the magnesium chloride hexahydrate into distilled water before mixing with magnesium oxide powder to produce MOC cement paste. The mass concentration of the solution is 217 g for 100 g of water.

3. Preparation of specimens

Magnesium oxide powder was mixed with magnesium chloride solution mechanically using a mixer (Heidolph RZR) to form homogenous MOC pastes. The weight of MgO is fixed and the weight of $MgCl_2.6H_2O$ has been varied.

Mixtures were cast in cylindrical molds (26 mm in diameter, 50 mm high) and stored for 24 h, then unmolded and air-cured for 28 days.

4. Measurements

The XRD analyzed was carried out on the powdered sample using X-Ray powder diffractometer (XRD PHILIPS) with Cu K radiation (λ K=1.54Å).

Differential thermograms were obtained using the Netzsch 449 STA F1 Jupiter thermal analys system. The rate of heating was 15°C / min.

The microstructure of the samples was examined using scanning electron microscope Carl ZEIIS LEICA S430i model.

Measurement of thermal conductivity was performed in dry state using Photothermal Deflection Technique. Setting time was determined by using Vicat Apparatus.

Porosity accessible to water of MOC is determined according to EN 12390-7 norm. The measurement of porosity in the water under a vacuum of 0.1 bar, quantify the volume of open pores (accessible to water) using the following protocol:

- Cement samples are placed in sealed desiccators and kept under Vacuum of 0.1 bar for 12 h.
- Previously degassed water is introduced progressively in desiccators to fill all the pores of samples, without introducing air bubbles.
- Once the samples are saturated, they kept immersed in water for 24 hours, and finally we determined hydrostatic mass m_{sss}^{imm} and saturated dry surface mass m_{ss}.

The porosity is calculated by the following equation (4):

$$\frac{m_{sss}-m_{dry}}{m_{sss}-m_{sss}^{imm}}$$

With:

m_{sss}: saturated dry surface mass of sample

m_{dry}: mass of sample before saturation

m_{sss}^{imm} : mass of sample measured in water

Table II: Experimental factors and levels investigated

Levels	Mass ratio of $MgCl_2/MgO$	Speed time (rpm)	Mixing time (min)
-1	1.42	650	5
0	1.82	1125	10
1	2.22	1600	15

RESULTS AND DISCUSSION

1. Studied factors and experimental domains

According to the preparation of MOC, 3 quantitative factors are chosen: mass ratio of $MgCl_2/MgO$, stirring speed and mixing time. The corresponding variables and their levels (set according to the data of preliminary experiments and the equipment abilities) are given in Table II. The two experimental responses tracked were compressive strength (Y_1) and the setting time (Y_2).

We should mention that we fixed H_2O\MgO mass ratio for each level.

To test the direct influence of the three studied factors as well as their possible interaction effects on the measured experimental responses, we have realized a two-level complete factorial design 2^3 which is expected to provide excellent information concerning not only the main effects but also the double interaction effects.

The experimental design and the measured responses are summarized in Table IV.

Comparing MOC and Portland cement (setting time between 2h and 3h), it is found that MOC has a faster setting. It also has better mechanical strength.

For a very short setting time (6 min), MOC have a high strength (75.48 MPa): in this case the cement is recommended for applications that require fast setting (decoration use, restoration of monuments, damaged marble ....).

For a longer setting time (64 min), also it has a good mechanical strength (46.59 MPa): in this case the cement is recommended for applications which require a longer setting time (floor covering ....).

Considering that the interaction effects between three or more factors are negligible, the factor effect estimation is computed [13] according to [14]:

$$b_i = \frac{\sum_j^N \pm Y_j}{N} \quad (5)$$

Where b_i is the effect estimation of the factor i, Y_j is the response j and N is the number of experiences.

The pooled variance estimation used to determine the significant factors is computed as

$$S_a^2 = \frac{\sum_i^n \nu_i S_i^2}{n} \quad (6)$$

Where S_a^2 is the pooled experimental variance, S_i^2 is the experimental variance estimation i, ν_i is the degree of freedom i and n= $\sum \nu_i$ is the degree of freedom of the pooled experimental variance.

2. Identification of the influential factors

Based on check student for an error risk α=5%, it was found that $t_{tabulated}$ = 4.303. Table V summarizes the factors effects estimation for the two responses: compressive strength (Y_1) and setting time (Y_2).

Table III: The mass ratio of H_2O\MgO

Levels	-1	0	1
H_2O\MgO	0.74	0.96	1.17

Table IV: Factorial matrix 2^3.

No. Exp.	Mass ratio of $MgCl_2/MgO$	Mixing time (min)	Stirring speed (rpm)	Compressive strength (MPa)	Setting time (min)
1	1.42	5	650	49.47	20
2	2.22	5	650	46.59	64
3	1.42	15	650	4.55	17
4	2.22	15	650	21.20	37
5	1.42	5	1600	41.38	14
6	2.22	5	1600	76.40	41
7	1.42	15	1600	75.48	6
8	2.22	15	1600	20.50	32
9	1.82	10	1125	67.00	30
10	1.82	10	1125	60.54	31
11	1.82	10	1125	59.00	28

Table V: Factors signification for the two responses Y_1 and Y_2

Coefficient	Y_1				Y_2			
	Value	SD	t.exp	P	Value	SD	t.exp	P
b_0	47.464	1.279	37.087	0.000726	29.090	0.460	63.1634	0.000251
b_1	-0.773	1.500	-0.515	0.657478	14.625	0.540	27.0802	0.001361
b_2	-11.513	1.500	7.672	0.016568	-5.875	0.540	-10.878	0.008345
b_3	11.493	1.500	7.658	0.016624	-5.625	0.540	-10.415	0.009093
b_{12}	-8.808	1.500	-5.869	0.027819	-3.125	0.540	-5.7864	0.028592
b_{13}	-4.216	1.500	-2.809	0.106780	-1.375	0.540	-2.5460	0.125809
b_{23}	6.063	1.500	4.040	0.056143	1.625	0.540	3.0089	0.094979
b_{123}	-13.691	1.500	-9.123	0.011802	2.875	0.540	5.3235	0.033522

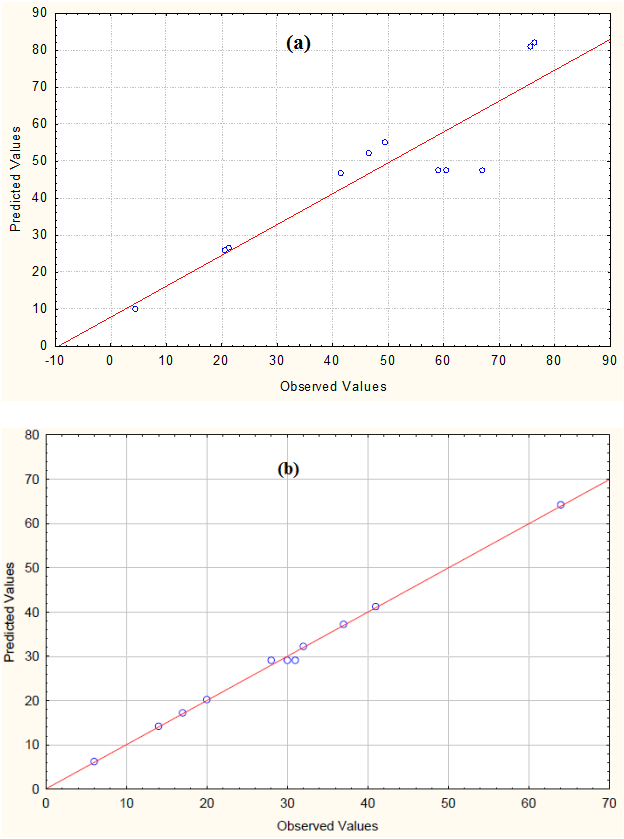

Figure 1: Calculated versus experimental values graph (a) for compressive strength (b) for setting time.

The two models are represented by the equations given below:

Compressive strength:

$$Y_{cal}1 = 47.464-11.513X_2+11.493X_3-8.808\ X_1X_2-13.6913\ X_1X_2X_3 \quad (7)$$

Setting time:

$$Y_{cal}2= 29.090+14.625X_1-5.875X_2-5.625X_3-3.125X_1X_2+2.875\ X_1X_2X_3 \quad (8)$$

3. Analysis of Residue

Figure 1 reveals the distribution of the calculated versus experimental values for the two responses (Y_1 and Y_2). The points are almost randomly distributed about the line representing exact agreement, providing good agreements between experimental values and those calculated using the model.

4. Analysis of Variance

Table VI summarizes the variance analysis of the chosen responses Y_1 and Y_2.

The main results for Y_1 and Y_2 are, respectively, 333.601 and 12.539, as lack of fit mean square and 18.017 and 2.333 as estimation of experimental variance. Thus, the values of the ratio between the lack of fit mean square and the estimation of experimental variance 18.51568 and 5.3739 for the responses Y_1 and Y_2 are inferior to tabled $F_{4,2}^{0.05}$ and $F_{3,2}^{0.05}$, respectively. Consequently, it is possible to confirm the validity of the two elaborated models. In addition, the ratios between the regression mean square and the residual mean square for the three responses Y_1 and Y_2 (4.638 and 5.3739) are superior to the tabled $F_{4,6}^{0.05}$ and $F_{5,5}^{0.05}$ respectively. Thus, the significant variables, applied to elaborate the three models, have a large significance on their responses.

5. Optimization

For selecting the optimal conditions we try to make a compromise between the two responses to have a good compressive strength and a suitable setting time.

By merely regarding values and signs of these significant effects, we conclude that maximization of the two responses is reached for experience number 6 (compressive strength = 76.40 MPa and setting time = 41 min):

- Mass ratio of $MgCl_2.6H_2O/MgO$ (X_1): 2.22
- Mixing time (X_2) : 5 min
- Stirring speed (X_3) : 1125 rpm

The phase diagram of the ternary MOC system (MgO-$MgCl_2$-H_2O) [5] at ambient temperature is

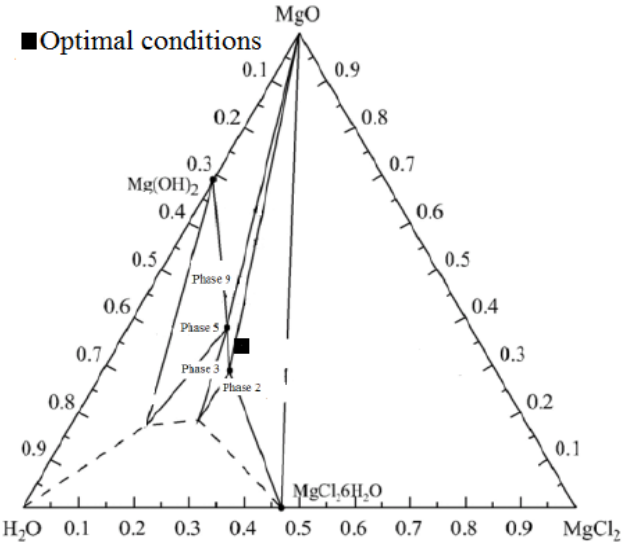

Figure 2: Phase diagram of the ternary MOC system

Table VI: Analysis of variance.

Source of variation	SS	DF	MS	Ratio	P
Compressive strength					
Regression	4237.738	4	1059.4345	4.63837	0.048
Residual	1370.437	6	228.40616		
Lack of fit	1334.403	4	333.601	18.51568	0.051897
Pure error	36,034	2	18.017		
Total	5608.174	10	1059.4345		
Setting time					
Regression	2384.625	5	476.925	56.40478	0.0000
Residual	42.277	5	8.4554		
Lack of fit	37.610	3	12.539	5.3739	0.160892
Pure error	4.667	2	2.333		
Total	2426.909	10	476.925		

illustrated in Figure 2 with the composition point of the optimum which is located near to the phase 5 responsible for the good compressive strength of the cement.

5. Characterization

Figure 3 shows the XRD pattern of MOC with optimal condition. It can be found that phase 5 is present. This phase is the major product responsible for hardening and the strength of MOC. We measured porosity accessible to water, we founded that the total porosity of MOC is 4% which is in a good accordance with other results in literature [15].

The thermal conductivity of cement is 0.8 w/ mK. The morphology of MOC is shown in Figure 4. We can see a rough surface with a dense network of needle-like crystals of 500 nm which has a high strength (Phase 5). Thermal analysis of MOC is shown in Figure 5. Six endothermic events appear on the DTA curves of MOC during heating. Thermal decomposition requires a dehydration stage of crystalline phase 5 $Mg(OH)_2$ $MgCl_2.8H_2O$ at 179°C to obtain an anhydrous materials. The other deflections in this curve at 358°C, 414°C, 484°C and 711°C present the decomposition stage

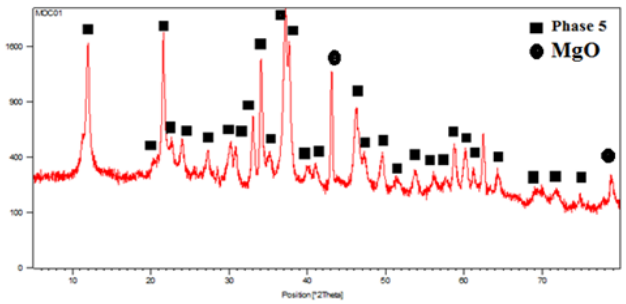

Figure3: XRD patterns of MOC

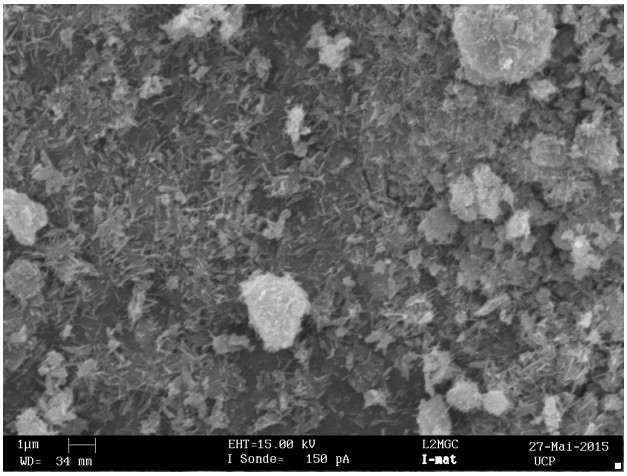

Figure 4: SEM analysis of MOC

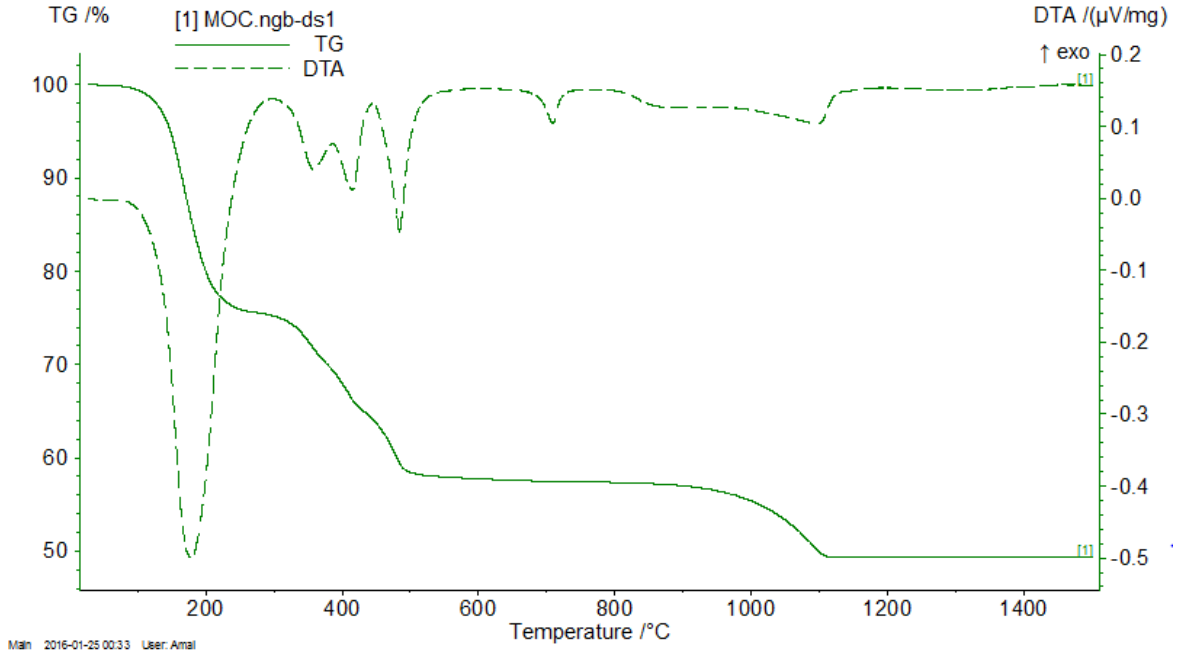

Figure 5: TG and DTA curves of MOC

of 5 $Mg(OH)_2 MgCl_2$ and the loss of $MgCl_2$. The last deflection at 1100°C
represents the decomposition to obtain the final solid product MgO.

CONCLUSION

The formation of MOC was carried out in this study using experimental design. The results showed that there is an agreement between the experimental values and those calculated from the model developed which confirms its validity. The optimal conditions are $MgCl_2.6H_2O/MgO$ (X_1): 2.22, Mixing time (X_2): 5 min and Stirring speed (X_3): 1125 rpm. The responses are: compressive strength = 76.40 MPa and setting time = 41 min. The interpretation of results found by DRX, IR, SEM and TG-DTA confirms the presence of phase 5 which is responsible for the good compressive strength of magnesium oxychloride cement.

ACKNOWLEDGEMENTS: This work was supported by a grant from Ministry of Higher Scientific Research of Tunisia. The authors would like to thank the technical team of the National Research Centre of Materials Sciences in Borj Cedria Technological Park and of L2MGC in University of Cergy-Pontoise.

REFERENCES

[1] G. Li, Y. Yu, J. Li, *Cons and Buil. Mat*, **2008**, 22, 521-525.
[2] JF. Montle, KG. Mayhan, J Fire Flammability/Fire Retard. Chem, **1974**, 1,243–54.
[3] R. Siddique, TR. Naik, *Waste Manage*, **2004**, 24, 563–9.
[4] H. Yu, Magnesium Oxychloride Cement and its Application, 1st ed., *China Building Materials Industry Press*, Beijing, **1993**.
[5] L, Zongjini, CK, Chau, *Cem. Concr. Res*, **2007**, 37,866-870.
[6] D.H. Deng, C.M. Zhang, *Cem. Concr. Res*, **1999**, 29, 1365–1371.
[7] Y. Li, H.F. Yu, J.M. Dong, J. Wen, Y.S, *J. Chin. Ceram. Soc*. **2013**, 41, 1465–1473.
[8] J. J, Beaudoin, V.S, Ramachandran, *Cem. Concr. Res* **1975**, 5, 617-630.
[9] C.Y. Wu, H.F. Zhang, H.F. Yu, *Adv. Cem. Res*. **2013**,25, 254–261.
[10] K. Xu, Y. Guo, Q. Sun, S. Dong, Z. Li, **2012**, 3, 1417–1428.
[11] D.H. Deng, C.M. Zhang, *Cem. Concr. Res*. **1996**, 26, 1203–1211.
[12] Y. Li, H. Yu, L. Zheng, J. Wen, C. Wu, Y. Tan, *Constr. Build. Mater*. **2013**, 38, 17.
[13] D.Mathieu, R.Phan Tan Luu , Nemrod-W Software. Aix-Marseille III University. France, **1999**.
[14] Goupy J, Modélisation par les plans d'expériences, *Techniques de l'ingénieur*. Traité Mesures et Contrôle pp1–23, **2000**.
[15] S. Zhao, J. Fan, W.Sun, *Constr. Build. Mater*, **2014**, 50, 540–548.